Ab Initio Quantum Chemical Studies of the Formaldiminoxy (CH_2NO) Radical: 2. Dissociation Reactions

Warwick A. Shapley and George B. Bacskay*

School of Chemistry, University of Sydney, NSW, 2006, Australia

Received: December 30, 1998; In Final Form: April 5, 1999

Following the theoretical work on the isomerization reactions of the formaldiminoxy (CH_2NO) radical, this paper reports the results of the ab initio quantum chemical study of the decomposition reactions of the various isomers, using the Gaussian-2 (G2), CASSCF, CASPT2, and QCISD(T) methods and basis sets that range from cc-pVDZ and cc-pVTZ to the 6-311+G(3df,2p) of G2. A total of 24 dissociation reactions of 11 isomers and their rotamers have been investigated. The lowest energy reactions occur for molecules with a NCO-chain backbone, which yield HCN, HNC, OH, NH_2, CO, HNCO, and H as primary products. The reaction that could compete with the above is the CH bond fission in CH_2NO, giving H + HCNO as products.

Introduction

The formaldiminoxy radical CH_2NO is generated mostly in the "reburning"[1−4] of nitric oxide by methylene during combustion. A quantum chemical study of the reactions governing its formation and isomerization has been reported in previous papers of ours,[5,6] as well as a paper by Roggenbuck and Temps.[7] In this paper we summarize the results of a detailed examination of the potential energy surfaces (PES) associated with the dissociation reactions of the various isomers of CH_2NO (I1−I11), as identified previously, which lead to a range of products: H, HCNO, HNCO, HONC, HCN, HNC, OH, NH_2, CO, NCO, CNO, and H_2. The results of this study provide information about the energetics and mechanisms of these elementary reactions which may be of benefit in future studies, especially in the development of realistic and reliable kinetic models of this system. Since many of the species are highly reactive intermediates with short lifetimes, the acquisition of experimental data is difficult, so theoretical studies such as ours may be the only source of thermodynamic and kinetic parameters.

Computational Methods

The procedures used in this work to characterize the stationary points on the PES for dissociative channels are the same as in our previous studies. Briefly, the energies of all isomers, transition states, and products were computed using the Gaussian-2 (G2) methodology.[8] The transition state energies were also computed at the CASPT2/cc-pVTZ and QCISD(T)/cc-pVTZ levels of theory, using geometries optimized at the CASSCF/cc-pVDZ level. In the CASSCF and CASPT2 calculations 11 electrons are treated as active in a space of 11 active orbitals, denoted 11/11. Since the transition states of the dissociation reactions involve bond fissions, CASSCF is expected to provide a more accurate description of such a process than MP2 (as used in G2).

Results and Discussion

As discussed in our previous papers,[5,6] the association reaction of triplet methylene and nitric oxide to give CH_2NO is exothermic by about 76.5 kcal/mol. If no thermal equilibration takes place, this energy could be used to facilitate subsequent isomerization and dissociation. Alternatively, what reactions CH_2NO may undergo will depend on the experimental conditions, viz. temperature and pressure.

The labeling of the isomers in the present work is the same as in our previous paper.[6] Similarly, the labeling of transition states continues on from that used previously. Unless indicated otherwise, the energies reported are relative to the ground-state energy of CH_2NO (I1).

The MP2/6-31G(d) and CASSCF(11/11)/cc-pVDZ geometries of the transition states that lead to products formed by a simple bond rupture in the CNO-chain and ring isomers are summarized in Figure 1, while those for the NCO-chain isomers are given in Figure 2. The structures of the transition states corresponding to hydrogen abstractions and HCN and CNO rearrangements are shown in Figure 3. The geometries of the final products are given in Figure 4. The absolute and relative G2, CASPT2, and QCISD(T) energies for the transition states are listed in Tables 1 and 2, respectively, while the absolute and relative G2 energies for the products are in Tables 3 and 4, respectively. In the discussion that follows we consider, in most instances, dissociations from only the most stable conformer of each isomer since the energy barriers associated with interconversion between conformers are generally much smaller than those associated with dissociations. The minimum-energy pathways of the dissociation reactions of the high-energy conformers are thus largely identical to those of their low-energy counterparts.

The dissociation reactions of isomers I1−I11 are discussed in the following sections.

1. CH_2NO (I1) → H + HCNO. This CH bond breaking reaction yielding atomic hydrogen and fulminic acid (HCNO) has been discussed previously in some detail.[5] The reaction is 53.7 kcal/mol endothermic at 0 K, as computed at the G2 level, with effectively no reverse barrier.

2. HCN(H)O (I2) → H + HCNO. When studied at the MP2 level, it was found that as the H−N bond is stretched the C-bound hydrogen swings around (in the molecular plane) to become cis to the leaving hydrogen in the transition state TS25, resembling the trans form of HCNO($^1A'$). (At both MP2 and CASSCF levels the predicted equilibrium structure of HCNO

* Corresponding author.

10.1021/jp9848187 CCC: $18.00
Published on Web 05/22/1999

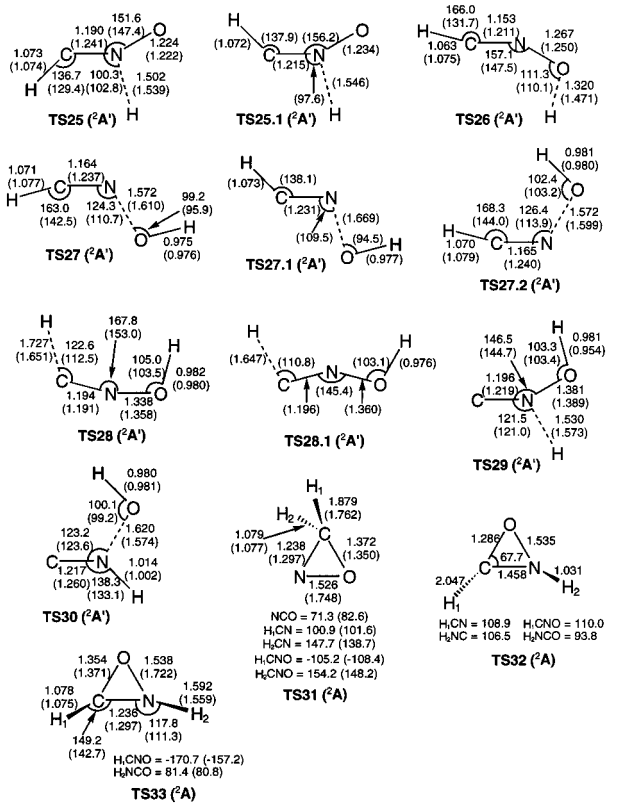

Figure 1. MP2/6-31G(d) geometries and CASSCF(11/11)/cc-pVDZ geometries (in parentheses) of species corresponding to transition states on the PES for the dissociation reactions of CNO-chain and ring isomers (in Å and deg).

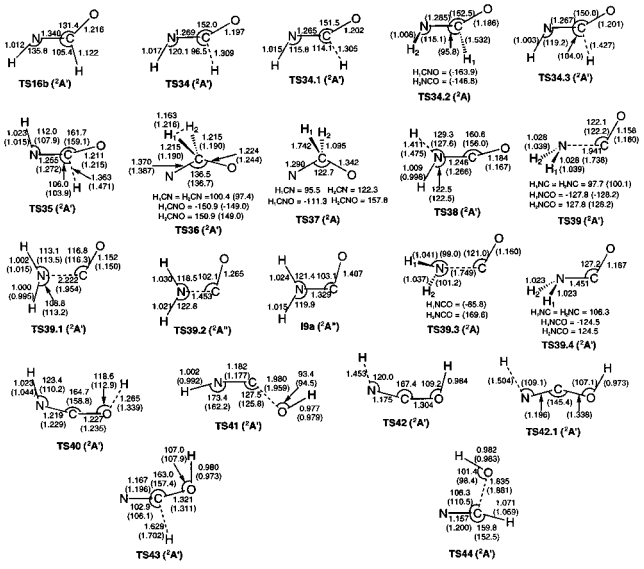

Figure 2. MP2/6-31G(d) geometries and CASSCF(11/11)/cc-pVDZ geometries (in parentheses) of species corresponding to transition states (and I9a) on the PES for the dissociation reactions of NCO-chain isomers (in Å and deg).

is slightly nonlinear.) The G2 barrier height was calculated to be 27.0 kcal/mol. However, this transition state actually connects both I2 and its geometric isomer I2a with H + HCNO. In fact, following the intrinsic reaction coordinate in the reverse direction from TS25 leads to I2a. At the CASSCF level the situation is somewhat different in that dissociation from I2 does proceed via a transition state in which the two hydrogens stay trans to each other (TS25.1). Once this barrier is passed, the

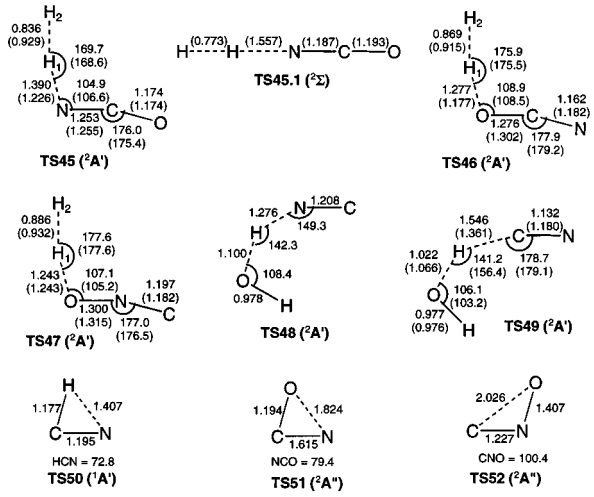

Figure 3. MP2/6-31G(d) geometries and CASSCF(11/11)/cc-pVDZ geometries (in parentheses) of species corresponding to transition states on the PES for the hydrogen abstractions and HCN and CNO isomerizations (in Å and deg).

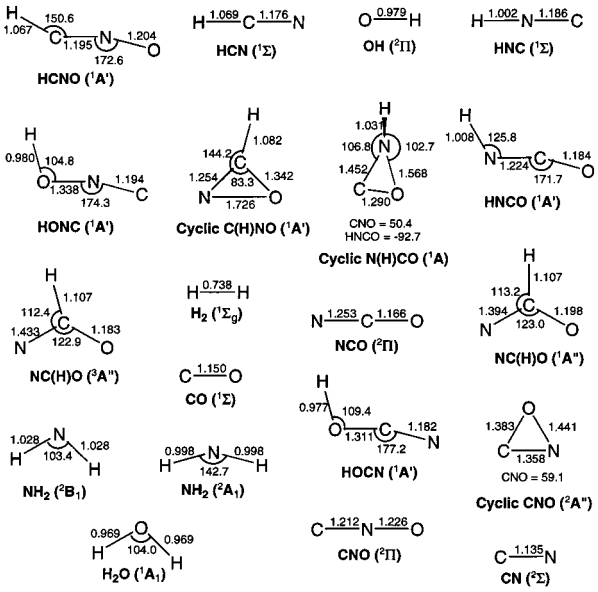

Figure 4. MP2/6-31G(d) geometries of species corresponding to stationary points on the PES for products formed from CH_2NO isomers (in Å and deg).

oxygen atom swings around to be cis to the leaving H, yielding again *trans*-HCNO as product. TS25 also exists at the CASSCF level and connects I2a with the dissociated products, in agreement with the MP2 results. Examination of the energies in Table 2 indicates that the energy barrier associated with TS25.1 is ~9 kcal/mol higher than for TS25, despite I2 being ~3 kcal/mol more stable than I2a. The critical energy of the rearrangement between I2 and I2a is expected to be ~6−10 kcal/mol (on the basis of similar rearrangements;[6] see, for example, TS5 and TS7) and thus the lowest energy decomposition pathway on the basis of the CASPT2 and QCI results is isomerization to I2a, followed by dissociation via TS25. Attempts to locate TS25.1 at the MP2 level consistently yielded TS25.

Loss of the C-bound H would lead to CN(H)O, a carbyne, with a very high energy. Attempts to locate a transition state for this reaction yielded the saddle point for the I2 → I4 interconversion (TS8) or the one corresponding to the loss of H from CH_2NO.[5]

TABLE 1: Electronic and Zero-Point Vibrational Energies of Transition States (and I1 and I1b) Associated with the Dissociation and Abstraction Reactions of CH_2NO[a]

	G2[b] (E_h)	ΔE_{ZPE}(G2) (kcal/mol)	CASPT2(11/11) cc-pVTZ (E_h)	QCISD(T) cc-pVTZ (E_h)	ΔE_{ZPE}(CASSCF(11/11)) (kcal/mol)
$CH_2NO(^2A')$ (I1)	−168.930 826	18.43	−168.928 014	−168.919 733	18.87
$TS25(^2A')$	−168.817 417	12.64	−168.806 114	−168.795 972	13.35
$TS25.1(^2A')$			−168.791 226	−168.780 921	12.83
$TS26(^2A')$	−168.826 206	12.16	−168.815 738	−168.805 657	12.96
$TS27(^2A')$	−168.892 172	16.40	−168.880 502	−168.876 906	16.26
$TS27.1(^2A')$			−168.878 179	−168.874 793	15.99
$TS27.2(^2A')$	−168.884 205	16.15	−168.873 043	−168.870 030	15.97
$TS28(^2A')$	−168.819 425	13.23	−168.802 416	−168.804 474	12.61
$TS28.1(^2A')$			−168.800 697	−168.804 727	12.66
$TS29(^2A')$	−168.804 679	13.53	−168.786 533	−168.784 588	13.59
$TS30(^2A')$	−168.867 340	17.24	−168.853 662	−168.853 604	17.04
$TS31(^2A)$	−168.798 488	13.94[c]	−168.793 441	−168.790 335	12.84
$TS32(^2A)$	−168.787 601	12.82			
$TS33(^2A)$	−168.799 982	11.87	−168.791 147	−168.788 342	12.41
$TS34(^2A')$	−168.947 493	13.87			
$TS34.1(^2A')$	−168.944 046	14.41			
$TS34.2(^2A)$			−168.923 791	−168.918 218	13.95
$TS34.3(^2A')$[d]			−168.928 972	−168.921842	13.32
$TS35(^2A')$	−168.931 094	14.43	−168.912 226	−168.908 051	14.15
$TS36(^2A')$	−168.829 386	14.26	−168.824 488	−168.810 221	13.28
$TS37(^2A)$	−168.783 796	12.60			
$TS38(^2A')$	−168.943 833	13.91	−168.928 166	−168.921 056	13.71
$TS39(^2A')$[d]	−168.956 459	17.75	−168.952 630	−168.951 520	16.73
$TS39.1(^2A')$[d]	−168.913 595	16.65[c]	−168.909 574	−168.908 185	15.90
$TS39.2(^2A'')$	−168.886 032	17.49			
$TS39.3(^2A)$			−168.953 075	−168.951 992	
$TS39.4(^2A')$	−168.977 579	19.46			
$TS40(^2A')$	−168.916 234	13.89	−168.899 746	−168.892 742	13.01
$TS41(^2A')$	−168.907 413	16.36	−168.897 536	−168.893 418	15.74
$TS42(^2A')$	−168.903 685	13.61			
$TS42.1(^2A')$			−168.876 979	−168.872 634	13.40
$TS43(^2A')$	−168.907 669	13.74	−168.894 663	−168.887 809	13.81
$TS44(^2A')$	−168.923 623	16.21	−168.914 451	−168.910 240	15.87
$TS45(^2A')$	−168.930 969	11.39	−168.912 403	−168.908 180	11.13
$TS45.1(^2\Sigma)$[e]			−168.844 654	−168.839 257	12.31
$TS46(^2A')$	−168.899 147	10.98	−168.878 190	−168.874 533	10.78
$TS47(^2A')$	−168.808 257	10.58	−168.781 749	−168.783 728	9.79
$TS48(^2A')$[f]	−168.881 635	12.49			
$TS49(^2A')$[f]	−168.905 751	12.11	−168.890 521	−168.886 984	12.50
$TS50(^1A')$	−93.214 989	6.51			
$TS51(^2A'')$	−167.621 973	3.12			
$TS52(^2A'')$	−167.626 400	3.62			
$TS53(^2B_2)$	−168.912 366	17.72			
$TS53.1(^2B_1)$[f]	−168.810 695	15.98			
$TS53.2(^2B_1)$	−168.796 658	17.00			
$TS54(^2A'')$[f]	−168.835 085	16.16			
$TS55(^2A')$	−168.791 609	13.66	−168.782 654	−168.774 786	13.86
$TS56(^2A')$	−168.971 173	19.32	−168.962 528	−168.959 118	19.15
$TS57(^2A')$[d,f]	−168.889 312	11.70	−168.871 942	−168.865 389	11.07
CH_2NO[g] (I1b)$(^2A')$	−168.877 734	17.48	−168.863 882	−168.863 495	16.84

[a] G2 energies at MP2/6-31G(d) geometries, CASPT2 and QCISD(T) energies at CASSCF(11/11)/cc-pVDZ geometries. [b] G2 energy includes the zero-point correction ΔE_{ZPE}(G2). [c] Using scaled MP2 frequencies. [d] Second-order saddle point at CASSCF level. [e] Third-order saddle point at CASSCF level. [f] Second-order saddle point at MP2 level. [g] Posesses an imaginary a″ frequency at CASSCF level.

3. HCNOH (I3) → H + HCNO/HCN + OH/H + HONC. No saddle point was found for the loss of the O-bound H from I3 at either MP2 or CASSCF levels of theory, suggesting the possible absence of a (reverse) barrier in that process. For the analogous reaction of I3a, a saddle point was located at both levels of theory (TS26), providing an upper bound of 65.7 kcal/mol (relative to $CH_2NO(^2A')$) for the critical energy associated with the formation of H + HCNO (P1/P1a) from any one of the three conformers of HCNOH. This corresponds to a reverse barrier height of ∼12 kcal/mol. (The barriers separating the three conformers are ∼6 kcal/mol.)

The dissociation of I3 to give $HCN(^1\Sigma)$ + $OH(^2\Pi)$ (P2) occurs via TS27, when studied by MP2. As the N−O length increases the C-bound H swings around to be cis to O so that at the saddle point the HCN angle is 163°. The G2 critical energy of this process is only 2.7 kcal/mol, with the reaction being ∼20 kcal/mol exothermic. Clearly, the N−O bond is very weak in HCNOH, as suggested by its length of 1.409 Å, whereas in TS27 it is only slightly longer at 1.572 Å, resulting in an "early" transition state with a low barrier. The rotamer I3b also dissociates via TS27, as indicated by the study of the recombination of HCN and OH which tends to produce I3b as product. When studied by CASSCF, I3 was found to dissociate via TS27.1 (a rotamer of TS27 which appears to be nonexistent at the MP2 level) where the C-bound H remains trans to O. Consequently, recombination of HCN and OH yields I3. TS27 was found at the CASSCF level, lying about 1 kcal/mol below TS27.1, but it connects only I3b with P2.

TABLE 2: G2, CASPT2, and QCISD(T) Energies (Including Zero-Point Correction) of Transition States (and I1b) Associated with the Dissociation and Abstraction Reactions of CH_2NO Isomers (Relative to CH_2NO ($^2A'$), in kcal/mol)[a]

	G2	CASPT2(11/11)/cc-pVTZ	QCISD(T)/cc-pVTZ	reaction
TS25($^2A'$)	71.17	70.97	72.14	I2, I2a → P1
TS25.1($^2A'$)		79.80	81.07	I2 → P1
TS26($^2A'$)	65.65	64.54	65.67	I3a → P1
TS27($^2A'$)	24.26	27.20	24.26	I3, I3b → P2
TS27.1($^2A'$)		28.39	25.32	I3 → P2
TS27.2($^2A'$)	29.26	31.59	28.29	I3a → P2
TS28($^2A'$)	69.91	72.55	66.07	I3 → P3
TS28.1($^2A'$)		73.68	65.96	I3 → P3
TS29($^2A'$)	79.16	83.50	79.52	I4 → P3
TS30($^2A'$)	39.84	44.83	39.67	I4 → P4
TS31(^2A)	83.04	78.42	75.17	I5 → P5
TS32(^2A)	89.88			I6 → P6
TS33(^2A)	82.11	79.43	75.99	I6 → P5
TS34($^2A'$)	−10.46			I7, TS16b → P7
TS34.1($^2A'$)	−8.30			I7b → P7
TS34.2(^2A)		−2.27	−3.97	I7 → P7
TS34.3($^2A'$)[b]		−6.15	−6.87	I7b → P7
TS35($^2A'$)	−0.17	5.19	2.61	I7a → P7
TS36($^2A'$)	63.65	59.37	63.13	I8 → P9
TS37(^2A)	92.26			I8 → P10
TS38($^2A'$)	−8.16	−5.26	−5.99	I9 → P7
TS39($^2A'$)[b]	−16.08	−17.59	−22.09	TS39.4 → P11
TS39.1($^2A'$)[b]	10.81	8.60	4.28	I9 → P11a
TS39.2($^2A''$)	28.11			I9a → P11
TS39.3(^2A)		−17.75	−22.26	I9 → P11
TS39.4($^2A'$)	−29.34			I9 → I9
TS40($^2A'$)	9.16	11.88	11.08	I10, I10a → P7
TS41($^2A'$)	14.69	16.00	13.38	I10 → P4
TS42($^2A'$)	17.03			I10, I10a → P12
TS42.1($^2A'$)		26.55	24.09	I10 → P12
TS43($^2A'$)	14.53	15.87	14.97	I11 → P12
TS44($^2A'$)	4.52	5.51	2.96	I11 → P2
TS45($^2A'$)	−0.09	2.06	−0.49	P7 → P9
TS45.1($^2\Sigma$)[c]		45.75	43.94	P7 → P9[d]
TS46($^2A'$)	19.88	23.18	20.27	P12 → P9
TS47($^2A'$)	76.91	82.70	76.26	P3 → P13
TS48($^2A'$)[e]	30.87			P4 → P14
TS49($^2A'$)[e]	15.73	17.16	14.18	P2 → P14
$OH(^2\Pi)$ + TS50($^1A'$)	45.13			P2 → P4
$H_2(^1\Sigma_g)$ + TS51($^2A''$)	89.42			P9 → P15
$H_2(^1\Sigma_g)$ + TS52($^2A''$)	86.64			P15 → P13
TS53($^2B_2$)	11.58			I1 → I1
TS53.1($^2B_1$)[e]	75.38			I1b → I1b
TS53.2($^2B_1$)	84.19			I1a → I1a
TS54($^2A''$)[e]	60.08			TS53 → I5
TS55($^2A'$)	87.36	86.21	85.95	I1b → P13
TS56($^2A'$)	−25.32	−21.38	−24.43	I9 → I9
TS57($^2A'$)[b,e]	26.05	27.39	26.30	TS56 → P9
CH_2NO (I1b)($^2A'$)[f]	33.32	38.21	33.26	

[a] G2 energies at MP2/6-31G(d) geometries, CASPT2 and QCISD(T) energies at CASSCF(11/11)/cc-pVDZ geometries. [b] Second-order saddle point at CASSCF level. [c] Third-order saddle point at CASSCF level. [d] Goes to the $^2\Sigma$ excited state of NCO. [e] Second-order saddle point at MP2 level. [f] Posesses an imaginary a″ frequency at CASSCF level.

The dissociation of I3a was also examined. The MP2 and CASSCF searches yielded effectively the same saddle point: TS27.2. Once again the C-bound H changes from being trans to O in I3a to cis in TS27.2 before assuming the linear HCN arrangement in the final products. This pathway, however, is energetically less favorable by ∼5 kcal/mol than the alternative mechanism of forming I3 or I3b followed by dissociation.

Production of H + HONC (isofulminic acid) ($^1A'$) (P3) from I3 is achieved by a simple rupture of the H−C bond. According to the MP2 results, as this H moves away it drags the C atom to the opposite side of the N−O bond so that in the transition state (TS28), the C and the O-bound H atoms become cis to each other, rather than trans, as in the reactant I3. Complete severing of the H−C bond, however, allows the carbon to bend back and adopt a trans HONC structure. TS28 is also the transition state for H loss by another conformation of HCNOH, namely where both hydrogens are in a cis configuration. As a result, recombination of H with HONC will, if the reaction stays on the minimum-energy path, lead to this higher energy conformer with a reverse barrier height of only 2.4 kcal/mol. CASSCF again predicts a somewhat different transition state for the I3 → P3 dissociation: TS28.1 which maintains the trans−trans configuration of I3. It is, however, essentially isoenergetic with TS28. While TS28 was successfully located at the CASSCF level, TS28.1 could not be found by MP2.

4. CN(H)OH (I4) → H + HONC/HNC + OH. Loss of the N-bound H from I4 yields H + HONC (P3). Both MP2 and CASSCF methods predict effectively the same transition state (TS29) for this process. The barrier to recombination, as computed by G2, has a height of 11.6 kcal/mol which is considerably higher than the 2.4 kcal/mol needed for the recombination to I3. Thus, on energetic grounds, the preferred

TABLE 3: G2 and Zero-Point Vibrational Energies of Products Formed from Isomers of CH_2NO[a]

	G2 (E_h)	ΔE_{ZPE}(G2) (kcal/mol)
HCNO($^1\Sigma$)	−168.345 292	12.88
HCNO($^1A'$)	−168.345 058	12.88
HCN($^1\Sigma$)	−93.284 89	10.08
HONC($^1A'$)	−168.323 159	12.57
HNC($^1\Sigma$)	−93.262 096	9.55
cyclic C(H)NO($^1A'$)	−168.321 555	11.71[b]
	−168.301 284[c]	11.79[d]
	−168.298 617[e]	
OH($^2\Pi$)	−75.643 91	5.10
cyclic N(H)CO(^1A)	−168.287 896	12.26
HNCO($^1A'$)	−168.456 771	12.77
NC(H)O($^3A''$)	−168.316 895	11.31
	−168.306 459[c]	11.49[d]
	−168.299 312[e]	
NCO($^2\Pi$)	−167.781 698	5.81
NC(H)O($^1A''$)	−168.302 633	11.25
NH_2($^2B_1$)	−55.789 02	11.52
NH_2($^2A_1$)	−55.737 858	11.70
CO($^1\Sigma$)	−113.177 49	3.11
H_2($^1\Sigma_g$)	−1.166 36	5.93
HOCN($^1A'$)	−168.416 250	13.18
CNO($^2\Pi$)	−167.681 385	5.28
CN($^2\Sigma$)	−92.582 76	4.03
H_2O($^1A_1$)	−76.332 05	20.51
cyclic CNO($^2A''$)	−167.660 294	4.34

[a] G2 energy includes the zero-point correction ΔE_{ZPE}(G2). [b] Using scaled MP2 frequencies. [c] CASPT2/cc-pVTZ//CASSCF/cc-pVDZ energy. [d] Using scaled CASSCF frequencies. [e] QCISD(T)/cc-pVTZ//CASSCF/cc-pVDZ energy.

TABLE 4: G2 Energies of Products Formed from Isomers of CH_2NO (Relative to CH_2NO ($^2A'$), in kcal/mol)

H + HCNO($^1\Sigma$)	(P1)	53.67
H + HCNO($^1A'$)	(P1a)	53.82
HCN($^1\Sigma$) + OH($^2\Pi$)	(P2)	1.27
H + HONC($^1A'$)	(P3)	67.56
HNC($^1\Sigma$) + OH($^2\Pi$)	(P4)	15.57
H + cyclic C(H)NO($^1A'$)	(P5)	68.57
		72.44[a]
		68.92[b]
H + cyclic N(H)CO(^1A)	(P6)	89.69
H + HNCO($^1A'$)	(P7)	−16.28
H + NC(H)O($^3A''$)	(P8)	71.49
		68.90[a]
		68.19[b]
H_2($^1\Sigma_g$) + NCO($^2\Pi$)	(P9)	−10.81
H + NC(H)O($^1A''$)	(P10)	80.44
CO($^1\Sigma$) + NH_2($^2B_1$)	(P11)	−22.39
CO($^1\Sigma$) + NH_2($^2A_1$)	(P11a)	9.71
H + HOCN($^1A'$)	(P12)	9.15
H_2($^1\Sigma_g$) + CNO($^2\Pi$)	(P13)	52.13
CN($^2\Sigma$) + H_2O($^1A_1$)	(P14)	10.05
H_2($^1\Sigma_g$) + cyclic CNO($^2A''$)	(P15)	65.37

[a] CASPT2/cc-pVTZ relative energy. [b] QCISD(T)/cc-pVTZ relative energy.

reaction between H and HONC is the formation of HCNOH rather than CN(H)OH.

Severing of the N−O bond results in the formation of HNC($^1\Sigma$) and OH($^2\Pi$) (P4). This reaction is exothermic by 26.4 kcal/mol at 0 K, at the G2 level. Since the N−O bond in I4 is likely to be very weak (r_{NO} = 1.444 Å), this dissociation reaction is expected to have a low barrier, comparable with that obtained for the analogous reaction of HCNOH (I3). The G2 barrier height corresponding to the MP2 saddle point (TS30) is in fact *negative* by 2.1 kcal/mol, suggesting that I4 may not be stable or that the barrier is very small but the corresponding saddle point geometry is not predicted accurately enough by MP2 theory. As a check, CASPT2 and QCI calculations were performed at the CASSCF geometries of both TS30 and I4.[6] These two calculations also predict TS30 to be more stable than I4, but only by ∼1 kcal/mol. These results indicate that I4 may not be predicted to be a stable molecule at the more highly correlated levels of theory, although it does correspond to a local minimum on the MP2 and CASSCF surfaces. Thus, the isomerization reactions of I2 and I3a that yield I4 as product could actually be dissociation reactions whereby the two reactions go to completion, yielding HNC + OH as effectively one step processes.

An isomer such as I4 may be thought of as a possible candidate to undergo a concerted reaction, resulting in CN + H_2O. No such transition state was, however, found. Thus, the only way of producing H_2O is by hydrogen abstraction by OH. Some of the possible reactions are discussed below. Abstractions, of course, require high concentrations of the radical species.

5. Cyclic CH_2NO (I5) → H + Cyclic C(H)NO. Breaking a C−H bond in I5 produces H plus the planar cyclic C(H)NO (oxazirine) ($^1A'$) molecule (P5). This reaction is endothermic by 53.7 kcal/mol and has a critical energy of 68.2 kcal/mol (corresponding to the transition state TS31) when computed by G2 at 0 K. According to CASPT2 and QCISD(T), the barrier may be 5−8 kcal/mol lower.

The possibility of concerted loss of H_2 from I5 to form cyclic CNO (P15) or NCO (P9) was investigated. The $^2A''$ state of I5 has five electrons in a″ MO's, whereas the $^2A''$ state of cyclic CNO and the $^2\Pi$ state of NCO in reduced (C_s) symmetry have only three such electrons. If one considers the reaction on the $^2A''$ surface, a possible transition state would have the partially formed H_2 molecule lying perpendicular to the CNO plane with the doubly occupied σ MO of H_2 being of a′ symmetry. Consequently, the number of a″ electrons must change from five to three during the course of the reaction and it is unlikely that a single reference treatment could describe it. Not surprisingly then, no such transition state was found at the MP2 level. The optimizations resulted in an excited $^2A''$ state of NCH_2O (I8), i.e., breaking the N−O bond. The CASSCF optimizations also failed in this case. The most likely scenario is, therefore, that H_2 elimination takes place via I8, which is a fairly low energy pathway (discussed below).

Another plausible dissociation channel that was tested is the simultaneous breaking of the C−N and C−O bonds to regenerate the original reactants CH_2 and NO. No transition state was found for such a reaction. The optimizations ended up producing saddle points connecting these products with either CH_2NO or CH_2ON. Accordingly, the minimum-energy path for the dissociation of I5 to methylene and nitric oxide is a two-step process requiring first a ring-opening reaction to one of the above isomers with subsequent dissociation of these.

6. Cyclic C(H)N(H)O (I6) → H + Cyclic N(H)CO/H + Cyclic C(H)NO. The second cyclic CH_2NO isomer I6 may undergo either a C−H or a N−H bond fission to yield two different cyclic isomers of HCNO. With regard to the former reaction, the G2 barrier height at TS32 of 51.8 kcal/mol is only marginally above the endothermicity of the reaction (51.6 kcal/mol) that yields H + cyclic N(H)CO (oxaziridinylidene) (^1A) (P6). At the CASSCF level this barrier disappears completely. Thus, any barrier to recombination, should it exist, would be negligibly small. Oxaziridinylidene, a cyclic carbene, is actually the least stable of all the products considered in this paper and thus its formation in any appreciable quantity is unlikely.

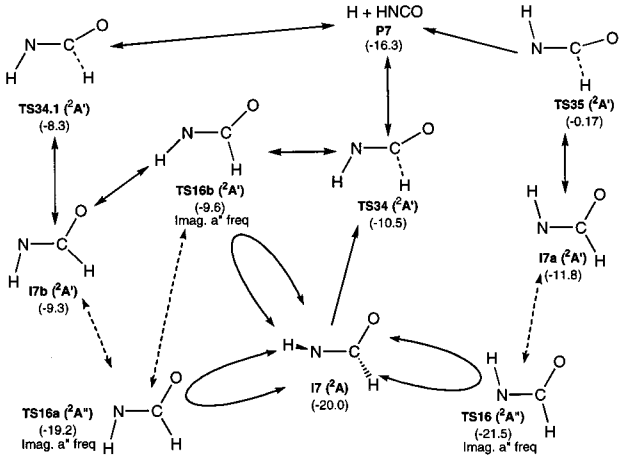

Figure 5. Reaction pathways for HNC(H)O dissociations to H + HNCO. Dashed lines represent transitions between the A′ and A″ surfaces. (The G2 energies in parentheses are relative to CH_2NO in kcal/mol.)

The second, substantially more stable, product formed from I6 is cyclic C(H)NO (^{1}A′) (P5). The transition state associated with this reaction is TS33. The G2 critical energy of this reaction is 44.1 kcal/mol, while the reaction is endothermic by 30.5 kcal/mol, making P5 the preferred product when I6 dissociates. The CASPT2 and QCI calculations actually suggest a lower barrier than G2, by ∼3−6 kcal/mol.

7. HNC(H)O (I7) → H + HNCO/H + NC(H)O. The potential surface describing the dissociation of HNC(H)O to H + HNCO (isocyanic acid) is rather more complex than for the reactions discussed previously since the planar conformers I7a and I7b are fairly close in energy to the nonplanar I7 with low barriers to their interconversion. Figure 5 summarizes the various pathways located on the G2 surface. If we consider initially a simple H−C bond fission of I7, we find that as the H is drawn away, the N-bound H rotates around the N−C bond so that the geometry of the transition state (TS34) has become planar with the HNCO moiety in a trans configuration. The barrier height at this point is 9.5 kcal/mol. Complete removal of the hydrogen then lowers the energy by 5.8 kcal/mol to yield H + HNCO (P7). For the association/recombination reaction of H with HNCO via TS34, which is planar, the reaction coordinate conserves planarity and rather than forming (nonplanar) I7, the product will be TS16b (^{2}A′) with an imaginary a″ frequency. To return to the original reactant I7, the C_s symmetry needs to be broken, which in reality is of course achieved by the coupling of the electronic and vibrational wave functions. (It should be pointed out, though, that while TS16b is of lower energy than TS34 at the MP2 level, its G2 energy is actually slightly higher.)

Although TS16b(^{2}A′) and I7b(^{2}A′) both have the same conformation, and similar energies as well as real a′ frequencies, the actual geometries in terms of bond lengths and angles are quite different. This is a consequence of the differences in their electronic structures. According to the SCF spin densities, the unpaired spin in TS16b resides predominantly on the N whereas in I7b it is largely on the O. TS16b is actually an excited state of TS16a(^{2}A″), which is also a transition state associated with the internal rotations in I7.

Dissociation of HNC(H)O may also occur from the planar I7a(^{2}A′) rotamer via TS35. Compared with the pathway that proceeds via TS34, this reaction has a significantly higher critical energy. The G2 energy at this point of −0.17 kcal/mol (relative to I1) is rather high and may be attributable in part to its cis HNCO conformation. Another possible route for the decomposition is via I7b (^{2}A′) and TS34.1. The geometry of the latter state is very similar to that of TS34, the greatest difference being a larger HCN angle in the former.

In summary then, at the G2 level the lowest energy pathway to P7 is a simple one-step bond-breaking reaction via TS34. A viable alternative is one proceeding via TS16a or TS16b to I7b and then via TS34.1 to H + HNCO. The highest energy on this pathway is (at −8.3 kcal/mol relative to CH_2NO) only marginally higher than the energy of TS34. Consequently, this mechanism could be of comparable importance with the first. The route via I7a appears less important as the highest barrier on this particular pathway is 8−10 kcal/mol above the critical energies encountered in the previous two mechanisms.

The mechanism for dissociation on the CASSCF PES is somewhat different from what occurs on the G2 PES primarily because of the existence of a nonplanar transition state (TS34.2) for the H−C bond breaking reaction of I7, although the energy of this transition state, when calculated by CASPT2 and QCI, is 6−8 kcal/mol greater than that of TS34. Moreover, these calculations suggest that the lowest energy pathway is one that passes through I7b and TS34.3, maintaining planar geometries, although at the CASSCF level both I7b and TS34.3 have imaginary a″ frequencies; i.e., their energies would decrease if allowed to become nonplanar. However, these calculations agree with G2 in that dissociation via such a cis-HNCO structure, such as I7a, is energetically less favorable, by 7−10 kcal/mol.

An alternative, much less favorable dissociation pathway for HNC(H)O, is the H−N bond fission, resulting in H + NC(H)O(^{3}A″) (P8) as products. This reaction is highly endothermic, with a G2 reaction energy of 91.5 kcal/mol. No saddle point could be located for this process, suggesting that there is no barrier to the recombination.

8. NCH_2O (I8) → H_2 + NCO/H + NC(H)O. The transition state (TS36) for the concerted elimination of H_2 from NCH_2O (^{2}A′) (I8) that occurs with the conservation of C_s symmetry, with NCO($^2\Pi$) (P9) as the other product, has been located by both MP2 and CASSCF methods. Furthermore, the reaction occurs without a change in the MO occupancy, since reactant, transition state, and product all have four a″ electrons. At the G2 level, the barrier to dissociation is only 6.9 kcal/mol, with the reaction being exothermic by 67.6 kcal/mol at 0 K. As discussed above, the expected pathway for the H_2 elimination reaction from cyclic CH_2NO(^{2}A″) (I5) is actually via I8 as intermediate.

With respect to H loss from I8, the MP2 and CASSCF calculations disagree as to the nature of the dissociation and the product formed. At the MP2 level, when searching for a saddle point, dissociation to H + NC(H)O(^{1}A″) (P10) is predicted, i.e., where one of the products (NC(H)O) is in an excited state. The barrier height at the transition state (TS37) and the endothermicity of the above reaction according to G2 are 35.5 and 23.6 kcal/mol respectively. The CASSCF calculations predict dissociation to H + NC(H)O(^{3}A″) (P8), without passing over a (reverse) barrier. At the CASSCF, CASPT2, and QCI levels of theory with the cc-pVTZ basis, the triplet state of NC(H)O, a nitrene, is predicted to be the ground state. Interestingly, the equilibrium geometry of the lowest ^{1}A′ state of C(H)NO is cyclic (P5). According to CASPT2 and QCI, this singlet state is above the triplet by 3.5 and 0.7 kcal/mol, respectively. By contrast, at the G2 level the singlet state is predicted to be 2.9 kcal/mol below the triplet. It has been recently noted by Sendt et al.[9] that G2 tends to underestimate the relative stabilities of triplet carbenes by ∼2.5 kcal/mol, while CASPT2 tends to overestimate them by as much as ∼4.8 kcal/

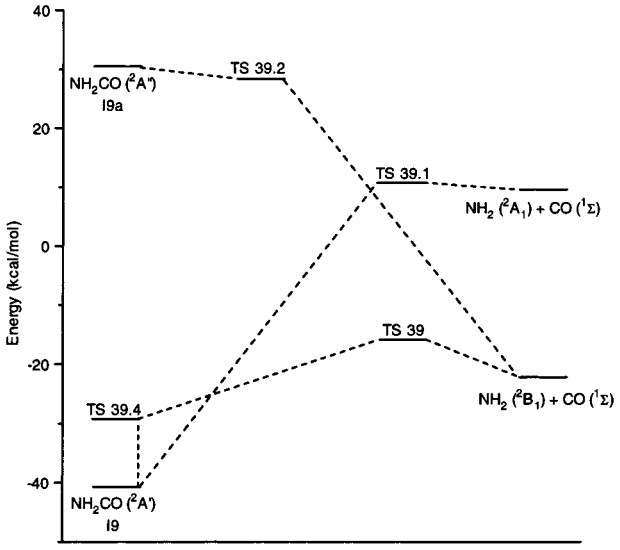

Figure 6. Schematic G2 potential energy surface for the dissociation of $NH_2CO(^2A')$ to $NH_2(^2B_1/^2A_1) + CO(^1\Sigma)$. (The energies are relative to CH_2NO.)

mol. It appears that for this unusual molecule the singlet and triplet states are near-degenerate, while their geometries are substantially different. In the decomposition reaction, therefore, the triplet channel, as predicted by CASSCF, is expected to be dominant, with the proviso that intersystem crossing to the lowest energy singlet surface is highly likely, given their near-degenerate energies.

9. NH_2CO (I9) → H + HNCO/NH_2 + CO/H_2 + NCO. The decomposition of NH_2CO (I9) to H + HNCO (P7) proceeds by a straightforward H−N bond fission with a barrier height at TS38 of 32.9 kcal/mol and an enthalpy of reaction (at 0 K) of 24.8 kcal/mol, when computed from G2 energies. According to the CASPT2 and QCI calculations, the barrier may be 2−3 kcal/mol higher. By contrast, the H−C bond fission in CH_2NO (I1) was found to have a reaction enthalpy of 53.7 kcal/mol and a very small or even nonexistent reverse barrier. Thus, H loss from I9 is significantly more favorable than from I1.

The most obvious dissociation channel for NH_2CO is to $NH_2(^2B_1)$ and $CO(^1\Sigma)$ (P11) as products. Indeed, among all the formaldiminoxy isomers and possible dissociation products, NH_2 and CO represent the third most stable state of this molecular system (after I9 and I11). However, since the ground state of NH_2CO correlates with the $^2A_1$ first excited state of NH_2 (P11a), surface crossing or loss of symmetry needs to take place as the reaction proceeds. A schematic PES, computed at the G2 level, is shown in Figure 6. Rather than considering the process of dissociation, it may be more instructive to examine the reverse process of association between NH_2 and CO in the C_s symmetry of the $NH_2\cdots CO$ supermolecule where the plane of symmetry is the molecular plane. Considering the ground $^2B_1$ state of this system, as the CN distance is decreased the energy rises, forming isomer I9a($^2A''$), which is an excited state of I9($^2A'$). According to G2, this reaction is endothermic by 52.8 kcal/mol. Using MP2, a transition state (TS39.2) was found for this process, but at the G2 level its energy falls slightly below that of I9a. If the G2 results are regarded as definitive, then the association of $NH_2(^2B_1)$ and CO on the $^2A''$ surface will be purely repulsive and I9a will not actually exist.

An alternative pathway that connects P11 with ground-state $NH_2CO(^2A')$ goes via TS39, although in this case the molecule becomes nonplanar, although of C_s symmetry, since the plane bisecting the HNH angle remains a reflection plane. The height of the barrier at TS39 is a modest 6.3 kcal/mol at the G2 level. If C_s symmetry is maintained, the product is TS39.4 which has an imaginary frequency corresponding to a symmetry-breaking rotation of the NH_2 group; i.e., it is a transition state associated with the internal rotation, with a critical energy of 11.7 kcal/mol. The lowest energy pathway is, however, expected to bypass TS39.4, i.e., allow the symmetry breaking to occur sooner and resulting in planar NH_2CO in its $^2A'$ ground state. The decomposition of NH_2CO is therefore expected to follow this pathway, by becoming nonplanar, passing through TS39, and resulting in the products NH_2 and CO in their respective ground states. According to the G2 calculations, the critical energy of this reaction is 25.0 kcal/mol while the reaction is endothermic by 18.7 kcal/mol at 0 K.

The CASSCF results provide a very similar description of the $NH_2CO \rightarrow NH_2 + CO$ reaction. The minimum-energy path is also one that breaks symmetry but unlike the MP2 transition state TS39, the corresponding CASSCF transition state is of C_1 symmetry, viz. TS39.3 (^2A), with TS39 predicted to be a second-order saddle point. The differences between the two geometries, TS39 and TS39.3, are quite small, and the effect of distortion to C_1 on the energy is ∼0.2 kcal/mol, when computed at the CASPT2 or QCI level of theory. Similarly, at the CASSCF level the planar TS39.1 also corresponds to a second-order saddle point.

The $NH_2CO \rightarrow H_2 + NCO$ reaction, which is found to be the least favorable of the three dissociation channels of NH_2CO, will be discussed in some detail in (13), following the discussion of the analogous H_2 elimination pathway from CH_2NO itself in (12).

The reaction of H with HNCO has been studied by Nguyen et al.,[10] who concluded that addition to the N center was the dominant entrance channel with NH_2 + CO the major decomposition products. Rate constant expressions for the production of NH_2 + CO and of H_2 + NCO from H + HNCO have also been determined, using statistical analysis, by Nguyen et al. and by Miller and Melius.[11] Both conclude that the former reaction is much faster than the latter. The predicted rate constants of both groups for the formation of NH_2 + CO agree well with that determined experimentally in a shock tube study by Mertens et al.[12]

10. HNCOH (I10) → H + HNCO/HNC + OH/H + HOCN. Breaking the H−O bond in HNCOH yields H + HNCO (P7). In this reaction, as the H−O bond is stretched, the molecule changes its conformation, such that in the transition state (TS40) the HNCO fragment changes to a cis configuration from the trans geometry of I10. A similar conformational change was noted in the case of the analogous H loss by HCNOH (I3). However, as the reaction proceeds, the conformation changes again, so that the product $HNCO(^1A')$ (P7) is in a trans configuration. TS40 is also the transition state for the decomposition of I10a. Indeed, if the reaction path for the recombination of H with HNCO is followed, after passing through TS40, it ends in I10a, which corresponds to the nearest local minimum, rather than in the global minimum I10. At the G2 level the barrier to reaction is 30.4 kcal/mol, with the reaction being endothermic by 4.9 kcal/mol. The CASSCF geometries and the CASPT2 and QCI energies are in reasonably close agreement with the G2 results.

Another dissociation channel leads to $HNC(^1\Sigma)$ and $OH(^2\Pi)$ (P4). Stretching the C−O bond results in the N-bound H becoming cis to O, as demonstrated by the geometry of the transition state (TS41). Past the barrier, the HNC fragment assumes a linear geometry. According to G2, which again is in

good agreement with the CASSCF-based results, the critical energy and reaction energy at 0 K are 35.9 and 36.8 kcal/mol, respectively, suggesting that there may not be a reverse barrier associated with this decomposition reaction.

The third decomposition pathway results in the formation of H + HOCN (cyanic acid) ($^1A'$) (P12). According to MP2, as the H−N bond is stretched, the conformation of the molecule changes such that the HOCN moiety is in a cis configuration. This is very similar to what happens during the H−O bond breaking reaction, as described above. The cis geometry is preserved in the transition state (TS42), but once over the barrier, HOCN resumes its trans configuration. Recombination along the minimum energy path (MEP) results in I10a. At the CASSCF level the all-trans geometry of HNCOH is preserved, so no conformational changes occur on either side of the barrier (TS42.1). The energies of the two transition states seem to differ by 7−10 kcal/mol. We expect the CASSCF based results to be the more reliable.

11. NC(H)OH (I11) → H + NC(H)O/H + NCOH/HCN + OH. No transition state was found for the direct dissociation NC(H)OH (I11) to H + NC(H)O($^3A''$ or $^1A''$) (P8 or P10). The searches led instead to TS23, the transition state associated with the isomerization of I11 to HNC(H)O (I7a), so it appears that the lowest energy decomposition path of I11 to H + NC(H)O is via this intermediate (I7a), which could then decompose to the above products. The overall reaction is computed to be endothermic by 95.4 kcal/mol. This reaction, however, is most unlikely to occur, since the decomposition to H + HNCO via I7 is only 7.7 kcal/mol endothermic, while the highest barrier in the process is 35.6 kcal/mol, corresponding to TS23.

Breaking the H−C bond in NC(H)OH yields H + HOCN. The transition state for this reaction is TS43, where the HOCN moiety is in a cis configuration, as in the reactant. At the G2 level the critical energy of this reaction is 38.5 kcal/mol, while the heat of the reaction at 0 K is 33.1 kcal/mol.

The third dissociation pathway results in the production of HCN($^1\Sigma$) and OH($^2\Pi$) (P2) which takes place via the transition state TS44, with a corresponding critical energy of 28.5 kcal/mol and an endothermicity of 25.2 kcal/mol at 0 K, as obtained by G2. This reaction is energetically the most favorable of those considered here as well as in comparison with the isomerization reactions.

12. CH_2NO (I1) → H_2 + CNO. As discussed in our previous paper,[5] no concerted H_2 elimination pathway was found from the ground state of CH_2NO. Elimination is possible, as shown by Roggenbuck and Temps,[7] if the molecule assumes a nonplanar geometry, corresponding to a $^2A'$ excited state, although these authors did not explicitly consider the process by which this state is accessed.

Our computed schematic G2 PES for this reaction is shown in Figure 7, while the geometries of the relevant species are given in Figure 8. Given that there are important changes in the (single reference) orbital occupancies of these species, the number of electrons occupying MO's of specific symmetries is also given (in square brackets) in the PES diagram for each system. Initially, the CNO angle opens up, with the three heavy atoms becoming linear and hence the molecule assuming C_{2v} symmetry at the saddle point TS53($^2B_2$), without any change in the MO occupancy. The height of the barrier is a modest 11.6 kcal/mol. Decreasing the CNO angle such that the CNO plane remains the reflection plane results in the formation of cyclic CH_2NO($^2A''$) (I5), via the transition state TS54, again without any changes in the MO occupancy. (Given that the reflection planes in I1 and I5 are perpendicular to each other,

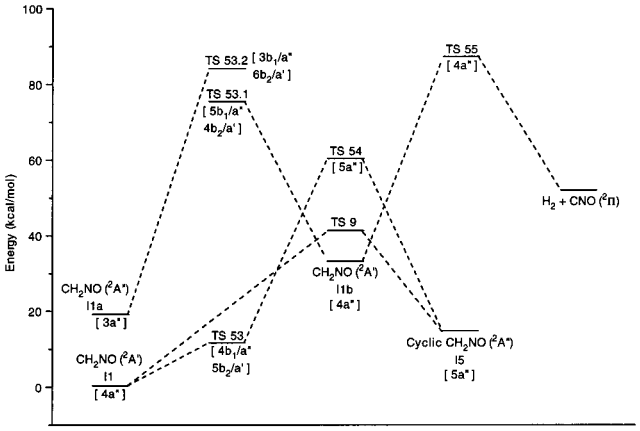

Figure 7. Schematic G2 potential energy surface for concerted elimination of H_2 from CH_2NO. (The energies are relative to CH_2NO.)

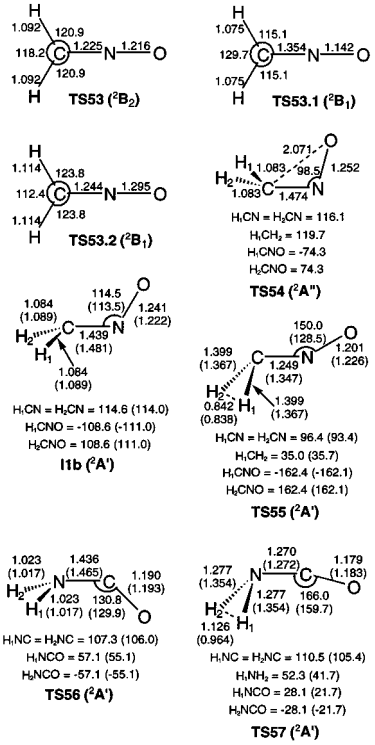

Figure 8. MP2/6-31G(d) geometries and CASSCF(11/11)/cc-pVDZ geometries (in parentheses) of species corresponding to stationary points on the PES for the concerted elimination of H_2 from CH_2NO and NH_2-CO (in Å and deg).

the symmetry labels a′ and a″ become interchanged for this I1→ TS53 → TS54 → I5 process.) However, as found before, I1 can cyclize in a one-step process by breaking the symmetry, going via the transition state TS9. As seen on the PES diagram in Figure 7, TS54($^2A''$) is an excited state of the desired intermediate I1b($^2A'$), while the latter effectively correlates with the $^2A''$ excited state of CH_2NO (I1a). Consequently, the lowest energy pathway from I1 to I1b would involve symmetry breaking and crossing from one diabatic surface to the other via an avoided crossing in the vicinity of TS9. We have not attempted to locate the position of the corresponding intersection. What is possibly more important, however, is that the dissociation of I1b takes place via the high-energy transition state TS55($^2A'$). The critical energy (relative to I1) is quite large at 87.4 kcal/mol, and thus this pathway is expected to contribute much less to the formation of H_2 than the alternative schemes described earlier.

At the CASSCF level the situation is different in that rather than being an equilibrium structure, I1b possesses an imaginary a″ frequency corresponding to the methylene torsion and thus it correlates with the planar CH_2NO isomer I1. Nevertheless, at the I1b geometry the $^2A'$ state (with four a″ electrons) has a lower energy than the lowest $^2A''$ state (with five a″ electrons). Thus, according to CASSCF, the reaction takes place largely in reduced (C_1) symmetry on the ground ^2A surface, although the mechanism for H_2 elimination is still basically the same, as it occurs via TS55. The latter is obviously the most important point on the PES with respect to the rate of formation of H_2 by this mechanism, and the CASPT2 and QCI methods both give essentially the same barrier height as G2.

13. NH_2CO (I9) → H_2 + NCO. In analogy with CH_2NO, no pathway was found for the concerted elimination of H_2 from the planar ground state of NH_2CO. The possibility of such a reaction occurring from a nonplanar $^2A'$ excited state, as found for CH_2NO, was therefore investigated. No analogous equilibrium structure to I1b was, however, found for such a state in the case of NH_2CO. Both trans and cis forms of $NH_2CO(^2A')$ (where the geometry was constrained to be of C_s symmetry, with the NCO plane bisecting the HNH angle) are first-order saddle points with imaginary a″ frequencies, i.e., transition states to the torsion about the N−C bond. Furthermore, the transition state actually associated with the H_2 elimination, viz. TS57-($^2A'$), is a second-order saddle point, with an imaginary a″ torsional frequency in addition to the one associated with the reaction coordinate. Allowing TS57 to break symmetry resulted in the transition state for H loss from planar NH_2CO (TS38) which lies ∼34 kcal/mol below TS57. Thus, H loss would be strongly favored over H_2 elimination, as in the case of CH_2NO itself.

Abstraction and Recombination Reactions. At sufficiently high radical concentrations, abstraction and recombination reactions may be a rich source of further bimolecular reactions and viable pathways for the formation of an increased range of products. Clearly, there are opportunities for much work in this area, but this would be best carried out within the framework of a kinetic model development which would provide information on the concentrations of the various species and hence an indication as to what bimolecular reactions may be worth considering. This is outside the scope of this work that includes only a small number of abstraction reactions as alternatives to unimolecular pathways to some simple products, but which could only be found by considering bimolecular processes. Thus, for example, $CN(^2\Sigma)$ and $H_2O(^1A_1)$ (P14) could result by H abstraction from HNC or HCN by OH, as an alternative to a concerted mechanism whereby CN(H)OH (I4) or NC(H)OH (I11) transfers the N-bound or C-bound H to the O while simultaneously breaking the N−O or C−O bond. We were unsuccessful in locating a transition state corresponding to such a process.

1. H + HCNO/HNCO/HOCN/HONC → H_2 + CNO/NCO/OCN/ONC. The first of these reactions, between H and HCNO, has been described in our previous work.[5] All these reactions seem to proceed in essentially the same manner with the abstracting hydrogen (H_2 in Figure 3) approaching the four-atom fragment from side-on. The transition states (TS45, TS46, and TS47 for the last three of these reactions) exhibit elongated H_1-H_2 and H_1-N or H_1-O bonds. The ground states of the various CNO isomeric products are $^2\Pi$. The (forward) barriers of these reactions are quite low at 16.2, 16.2, 10.7, and 9.4 kcal/mol, respectively, when computed at the G2 level. As for the H + HCNO reaction, the barrier for the H + HNCO reaction at a linear geometry (i.e., on the $^2\Sigma$ surface) is considerably higher in both absolute and relative terms. At the CASSCF level the transition state (TS45.1) for this reaction is actually a third order saddle point with imaginary (degenerate) bending frequencies in addition to the imaginary frequency associated with the reaction coordinate. The same conclusions would also apply to the H abstractions from HOCN and HONC at linear geometries, since NCO and CNO would necessarily form in their $^2\Sigma$ excited states.

2. HNC/HCN + OH → CN + H_2O. As remarked above, H_2O and CN (P14) could result from the abstraction of H from either HNC or HCN by OH, although these reactions would be of importance in a combustion process only if the reactant concentrations were sufficiently high. The reactions for HNC and HCN proceed via transition states TS48 and TS49, respectively, producing CN and H_2O in their ground states. At the MP2 level these two (planar) transition states are actually second-order saddle points with an imaginary out-of-plane bending frequency in addition to the one associated with the reaction coordinate. Attempts to locate the true nonplanar transition states at the MP2 level were unsuccessful. Using CASSCF, a saddle point geometry for TS49 was found, corresponding to a planar structure. The three computational methods predict quite similar values for the critical energy, ∼15 kcal/mol (relative to HCN + OH), which is comparable with the corresponding G2 estimate of 15.3 kcal/mol for the HNC + OH reaction. These abstraction reactions were also studied by Palma et al.,[13] using multireference CI techniques and a 6-311+G(d,p) basis. The analogous critical energies as calculated by these authors were significantly higher at 28.6 and 35.3 kcal/mol. Given the level of consistency among the G2, CASPT2, and QCISD(T) energies, as well as the more extensive basis sets used in this study, we expect our results to be more reliable.

Unfortunately, we were unsuccessful in our initial attempts to find the CASSCF geometry for TS48, but as this reaction is of minor importance we did not persevere. Whereas we estimate the barrier heights for the two individual forward reactions as being quite close, the barrier heights for the reverse process of abstraction of H from H_2O by CN differ by nearly a factor of 4, suggesting that the formation of HCN via TS49 will be the preferred channel.

Reactions of Primary Products. Once a dissociation reaction has occurred, it could be followed by isomerizations and dissociations of the products. The most extensive of these are the reactions of HCNO and its isomers. These have been extensively studied already, most recently by Mebel et al.,[14] who used density functional theory in a detailed characterization of the lowest singlet and triplet potential energy surfaces of HCNO. Comparison of their results with G2 predictions and the characterization of additional isomerization pathways are the subject of a forthcoming publication of ours.[15]

Another important class of reactions are those of the HCN and NCO species. As to the former, it is well-known that HCN and HNC can readily interconvert by simple transfer of the H via TS50. The G2 value of 43.9 kcal/mol for the critical energy compares favorably with the value of 44.6 kcal/mol of Lee and Rendell,[16] obtained in an extensive CCSD(T) study. Therefore, this mechanism is expected to play a significant role in determining the relative abundances of these two species. Furthermore, as shown by Talbi and Ellinger,[17] H atoms could efficiently catalyze this interconversion, since the forward and reverse critical energies for the exchange reaction

$$H + CNH \leftrightarrow HCNH \leftrightarrow HCN + H$$

TABLE 5: Summary of the G2 Energetics (in kcal/mol) of the Dissociation Reactions of CH_2NO (Including Also the Appropriate Isomerization Pathways that Precede Dissociation)

0	CH_2NO (I1)	→			$CH_2 + NO$										
	0.0				76.5										
1	CH_2NO (I1)	→			H + HCNO (P1)										
	0.0				53.7										
2	CH_2NO (I1)	→	TS1	→	HCN(H)O (I2)	→	TS25	→	H + HCNO (P1)						
	0.0		76.1		44.2		71.2		53.7						
3a	CH_2NO (I1)	→	TS4	→	HCNOH (I3)	→	TS26	→	H + HCNO (P1)						
	0.0		80.3		21.5		65.7		53.7						
3b					HCNOH (I3)	→	TS27	→	HCN + OH (P2)						
					21.5		24.3		1.3						
3c					HCNOH (I3)	→	TS28	→	H + HONC (P3)						
					21.5		69.9		67.6						
4	CH_2NO (I1)	→	TS1	→	HCN(H)O (I2)	→	TS8	→	CN(H)OH (I4)	→	TS29	→	H + HONC (P3)		
	0.0		76.1		44.2		67.7		41.9		79.2		67.6		
5	CH_2NO (I1)	→	TS9	→	cycl CH_2NO (I5)	→	TS31	→	H + cycl C(H)NO (P5)						
	0.0		41.3		14.9		83.0		68.6						
6a	CH_2NO (I1)	→	TS9	→	cycl CH_2NO (I5)	→	TS10	→	cycl C(H)N(H)O (I6)	→	TS32	→	H + cycl N(H)CO (P6)		
	0.0		41.3		14.9		77.5		38.1		89.9		89.7		
6b									cycl C(H)N(H)O (I6)	→	TS33	→	H + cycl C(H)NO (P5)		
									38.1		82.1		68.6		
7	CH_2NO (I1)	→	TS9	→	cycl CH_2NO (I5)	→	SC13	→	NCH_2O (I8)	→	TS14	→	HNC(H)O (I7)	→	
	0.0		41.3		14.9		58.4		56.8		55.9		−20.0		
									HNC(H)O (I7)	→	TS34	→	H + HNCO (P7)		
									−20.0		−10.5		−16.3		
8a	CH_2NO (I1)	→	TS9	→	cycl CH_2NO (I5)	→	SC13	→	NCH_2O (I8)	→	TS36	→	H_2 + NCO (P9)		
	0.0		41.3		14.9		58.4		56.8		63.7		−10.8		
8b									NCH_2O (I8)	→	TS37	→	H + NC(H)O (P10)		
									56.8		92.3		80.4		
9a	CH_2NO (I1)	→	TS9	→	cycl CH_2NO (I5)	→	SC13	→	NCH_2O (I8)	→	TS14	→	HNC(H)O (I7)	→	
	0.0		41.3		14.9		58.4		56.8		55.9		−20.0		
					HNC(H)O (I7)	→	TS15	→	NH_2CO (I9)	→	TS38	→	H + HNCO (P7)		
					−20.0		9.7		−41.1		−8.2		−16.3		
9b									NH_2CO (I9)	→	TS39	→	NH_2 + CO (P11)		
									−41.1		−16.1		−22.4		
9c									NH_2CO (I9)	→	TS57	→	H_2 + NCO (P9)		
									−41.1		26.1		−10.8		
10a					HNC(H)O (I7)	→	TS19	→	HNCOH (I10)	→	TS40	→	H + HNCO (P7)		
					−20.0		13.3		−21.2		9.2		−16.3		
10b									HNCOH (I10)	→	TS41	→	HNC + OH (P4)		
									−21.2		14.7		15.6		
10c									HNCOH (I10)	→	TS42	→	H + HOCN (P12)		
									−21.2		17.0		9.2		
11a					NCH_2O (I8)	→	TS20	→	NC(H)OH (I11)	→	TS23	→	HNCOH (I7a)	→	
					56.8		60.1		−23.9		11.7		−11.8		
									HNC(H)O (I7a)	→			H + NC(H)O (P10)		
									−11.8				80.4		
11b									HNC(H)O (I7a)	→	TS43	→	H + HOCN (P12)		
									−11.8		14.5		9.2		
11c									HNC(H)O (I7a)	→	TS44	→	HCN + OH (P2)		
									−11.8		4.5		1.3		
12	CH_2NO (I1)	→	TS55	→	H_2 + CNO (P13)										
	0.0		87.4		52.1										

were calculated by them to be quite low: 4.2 and 17.8 kcal/mol, respectively.

CNO may also isomerize, to cyclic CNO($^2A''$) and then to NCO. Cyclic CNO is connected to NCO and CNO by TS51 and TS52, respectively, both of which are quite high-energy saddle points on the PES. Therefore, this mechanism is not expected to play an important role in determining the production of NCO and CNO, although we note that H_2 + cyclic CNO is by no means the most energetically unfavorable product.

Summary of Dissociation Reaction Pathways. The reaction pathways to dissociated products are summarized in Table 5 and Figure 9, where the solid lines represent the minimum-energy route and dashed lines represent higher energy alternatives. The reactions where no transition states are specified, i.e., CH_2 + NO, H + HCNO and H_2 + CNO, were the subject of our previous study.[5] The initial step is the association of methylene and nitric oxide to give CH_2NO which is exothermic by 76.5 kcal/mol. Formation of other CNO-chain isomers involves a barrier of 76.1 kcal/mol and therefore formation of the NCO-chain and ring isomers is energetically more favorable. These reactions are unimolecular and therefore not dependent on the concentrations of the reacting species in the combustion system. Alternative, lower energy routes to I2, I3, and I4 do exist, although these proceed via dissociation/recombination and as such they are not viable unless concentrations of the intermediate dissociated species are quite high. Accordingly, the assumption is made that only unimolecular isomerizations occur, for which the appropriate barrier heights (i.e., those of TS1, TS9, and TS13) are to be used.

An examination of the results in Table 5 and Figure 9 allows us to make a number of general observations. For the majority of products more than one pathway to their formation exists. Moreover, these pathways are often of similar energy. The highest energy products, mostly H and high-energy isomers of HCNO, not surprisingly have the highest energy barriers, specifically P3, P5, P6, P8, P10, and P15. Concerted loss of H_2

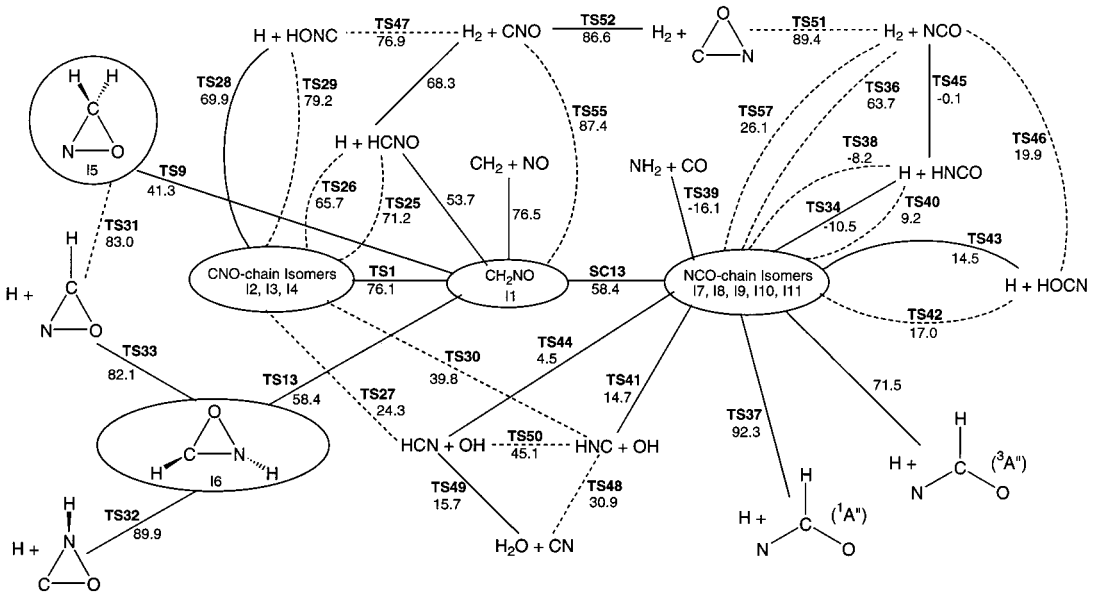

Figure 9. Reaction pathways for dissociations. Full lines represent the minimum energy path, dashed lines represent higher energy alternatives. (The G2 energies of transition states are relative to CH_2NO in kcal/mol.)

is most likely to proceed from NH_2CO (I9) via TS57, although its formation from NCH_2O (I8) via TS36 is likely to be a viable alternative, given that I8 is a common intermediate in both pathways. Both mechanisms generate NCO in the process. Formation of CNO in appreciable quantities is unlikely since the barriers connecting it with NCO and CH_2NO are quite high. The lower-energy abstraction route involving HCNO would be feasible only if high concentrations of reactants were present. As discussed above, H_2O can only be formed by an abstraction involving P2 or P4 so that while energetically accessible pathways exist, production of P14 is not expected to be great under normal conditions.

The lowest energy pathway leads to the direct formation of H + HCNO from CH_2NO. This is in agreement with the recent room temperature work of Grussdorf et al.[18] on the $^3CH_2$ + NO reaction, who found that the main product (~84%) is HCNO with a second channel (~15%) leading to HCN. According to our work, the lowest energy pathway to HCN is via the isomerization of HNC which comes from the decomposition of HNCOH (I10). Given that the lowest energy source of I10 is HNC(H)O (I7), we would expect that the dissociation products of I7 and I10 would occur in comparable quantities, i.e., that in addition to HCN, comparable quantities of HNCO, NH_2, CO, and HOCN would be also observed. Only CO was reported as having been detected in the experiments of Grussdorf et al.[18] Clearly, a kinetic modeling study of these reactions is needed to allow more meaningful comparisons to be made between theory and experiment and to resolve any apparent discrepancies.

Conclusions

Within the framework of the extensive ab initio study reported in this paper, the potential energy surface of the formaldiminoxy system was systematically explored, resulting in the identification and characterization of a number of pathways that contribute to the overall decomposition of this molecule. Given the high stability of the NCO-chain isomers and the relatively low energy that is required to isomerize CH_2NO to species such as NH_2-CO, NC(H)OH, HNCOH, and HNC(H)O, decomposition of these to yield HCN, HNC, OH, NH_2, CO, HNCO, and H appears very favorable. By contrast, the isomerizations among the CNO-chain isomers, as well as their dissociation reactions, are generally more energetic and therefore they are not expected to compete strongly with those of the NCO species, with the possible exception of the decomposition channel $CH_2NO \rightarrow H + HCNO$. Secondary reactions, such as abstractions by H, are energetically quite favorable and could well be of importance. While the data generated in this work is expected to be of value in the study of combustion reactions and atmospheric chemistry, its real value and accuracy can only be assessed by testing its performance in a realistic kinetic model.

Acknowledgment. The award of a Sydney University Postgraduate Scholarship to W.A.S. is gratefully acknowledged.

References and Notes

(1) Wendt, J. O. L.; Sternling, C. V.; Matovich, M. A. In *14th Symposium (International) on Combustion*; The Combustion Institute: Pittsburgh, PA, 1973; p 897.

(2) Myerson, A. L. In *15th Symposium (International) on Combustion*; The Combustion Institute: Pittsburgh, PA, 1975; p 1085.

(3) Song, Y. H.; Blair, D. W.; Siminski, V. J.; Bartok, W. In *18th Symposium (International) on Combustion*; The Combustion Institute: Pittsburgh, PA, 1981; p 53.

(4) Chen, S. L.; McCarthy, J. M.; Clark, W. D.; Heap, M. P.; Seeker, W. R.; Pershing, D. W. In *21st Symposium (International) on Combustion*; The Combustion Institute: Pittsburgh, PA, 1986; p 1159.

(5) Shapley, W. A.; Bacskay, G. B. *Theor. Chem. Acc.* **1998**, *100*, 212.

(6) Shapley, W. A.; Bacskay, G. B. *J. Phys. Chem. A* **1999**, *103*, 4505.

(7) Roggenbuck, J.; Temps, F. *Chem. Phys. Lett.* **1998**, *285*, 422.

(8) Curtiss, L.; Raghavachari, K.; Trucks, G.; Pople, J. *J. Chem. Phys.* **1991**, *94*, 7221.

(9) Sendt, K.; Ikeda, E.; Bacskay, G. B.; Mackie, J. C. *J. Phys. Chem. A* **1999**, *103*, 1054.

(10) Nguyen, M. T.; Sengupta, D.; Vereecken, L.; Peeters, J.; Vanquickenborne, L. G. *J. Phys. Chem.* **1996**, *100*, 1615.

(11) Miller, J. A.; Melius, C. F. *Int. J. Chem. Kinet.* **1992**, *24*, 421.

(12) Mertens, J. D.; Kohse-Höinghaus, K.; Hanson, R. K.; Bowman, C. T. *Int. J. Chem. Kinet.* **1991**, *23*, 655.

(13) Palma, A.; Semprini, E.; Stefani, F.; Talamo, A. *J. Chem. Phys.* **1996**, *105*, 5091.

(14) Mebel, A. M.; Luna, A.; Lin, M. C.; Morokuma, K. *J. Chem. Phys.* **1996**, *105*, 6439.

(15) Shapley, W. A.; Bacskay, G. B. *J. Phys. Chem. A*, manuscript submitted.

(16) Lee, T. J.; Rendell, A. P. *Chem. Phys. Lett.* **1991**, *177*, 491.

(17) Talbi, D.; Ellinger, Y. *Chem. Phys. Lett.* **1996**, *263*, 385.

(18) Grussdorf, J.; Temps, F.; Wagner, H. Gg. *Ber. Bunsen-Ges. Phys. Chem.* **1997**, *101*, 134.